International Journal of Earth Sciences
https://doi.org/10.1007/s00531-018-1623-9

ORIGINAL PAPER

Tectonothermal analysis of a major unit of the Cantabrian Zone: the Ponga unit (Variscan belt, NW Spain)

Susana García-López[1] · Gustavo G. Voldman[1,2] · Fernando Bastida[1] · Jesús Aller[1]

Received: 29 December 2017 / Accepted: 31 May 2018

Abstract
The paleothermometric evolution of the Ponga unit at the core of the Cantabrian Zone, the arcuate foreland fold and thrust belt of the Variscan orogen in NW Spain, is analyzed using the conodont Color Alteration Index and the Kübler Index of illite. The results indicate that the distribution of the thermal maturity patterns is independent of the stratigraphy and the structure of the unit. These include the occurrence of dominant diagenetic values and very low-to-low-grade metamorphism in the southern area. The main thermal event is interpreted to be related to hydrothermal fluids ascending through late-Variscan extensional faults. The anomalous high heat flow in the southern sector of the Ponga unit is part of a previously identified large band in the Cantabrian Zone, where the common occurrence of low-grade metamorphic rocks, hydrothermal dolostones, and ore mineralizations is related to an extensional orogenic episode that started near the Carboniferous–Permian boundary, soon after the closure of the Asturian arc.

Keywords Diagenesis-metamorphism · CAI · KI · Hydrothermalism · Variscan · Paleozoic · NW Spain

Introduction

The Cantabrian Zone (CZ) is the foreland fold and thrust belt of the Variscan orogen in the northwestern Iberian Peninsula, and constitutes an ideal setting to analyze the tectonothermal evolution of the external areas of an arcuate orogenic belt (Fig. 1). It presents a near complete stratigraphic succession from the Cambrian to the upper Carboniferous, with only important gaps in some areas, such as the Ponga area. The succession of the CZ has been divided into two tectonostratigraphic sequences (Julivert 1978; Marcos and Pulgar 1982): a pre-orogenic sequence, which is wedge-shaped tapering towards the foreland, and a syn-orogenic sequence, including several clastic wedges in front of the main thrust units. The contact between the two sequences is close to the Devonian–Carboniferous boundary. The CZ presents thin-skinned structural style with large thrust units and associated folds. In most of this thrust and fold belt, the Variscan deformation took place under diagenetic conditions. However, very low- or low-grade metamorphism is reached in local areas, which have been associated with various processes, such as burial, orogenic, hydrothermal, and contact thermal events (Valín et al. 2016 and references therein).

Several paleothermometric studies have pursued deciphering the tectonothermal evolution of the CZ. Most of them are based on the conodont Color Alteration Index (CAI) and the Kübler Index (KI), as well as clay minerals, coal rank, fluid inclusions, and vitrinite reflectance. Tectonothermal studies using CAI and/or KI in the western, northwestern, and southwestern parts of the CZ show the transition from diagenesis to orogenic metamorphism towards the hinterland, which is located to the west of the CZ (Pérez-Estaún 1978; Aller et al. 1987; Gutiérrez-Alonso and Nieto 1996; García-López et al. 1997; Brime et al. 2001). Cleavage development is associated with this transition.

The previous studies have shown that the main thrust units of the southern and western parts of the CZ present a paleotemperature increase toward the basal part of the units, where anchizonal/ancaizonal conditions are occasionally reached. This thermal trend is disrupted by the basal thrust of the units, indicating that the boundary of the unit is also a thermal boundary. This also indicates that the thermal peak

✉ Gustavo G. Voldman
gvoldman@unc.edu.ar

[1] Departamento de Geología, Universidad de Oviedo, 33005 Oviedo, Spain

[2] CICTERRA (CONICET-UNC), CIGEA, X5016GCB Córdoba, Argentina

Published online: 18 June 2018

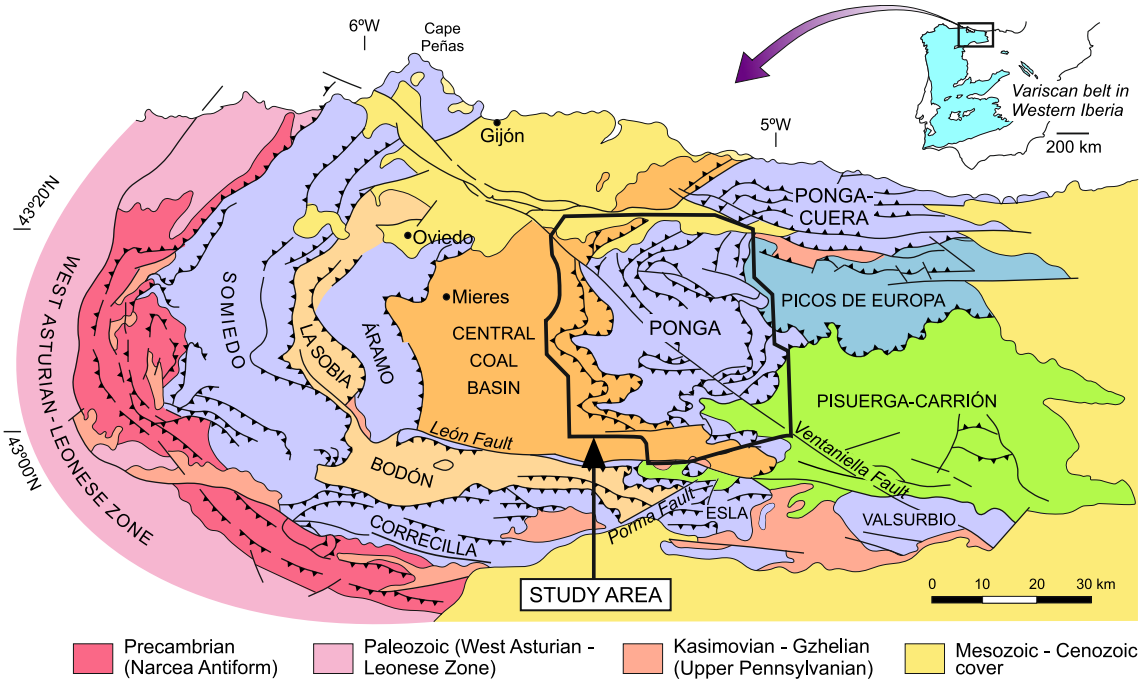

Fig. 1 Schematic geological map of the Cantabrian Zone (modified from Julivert 1971) showing major Paleozoic thrust units and the location of the study area

occurred prior to the cessation of emplacement of the thrust sheets and that the heating is due to burial (Aller et al. 1987, 2005; Bastida et al. 1999; García-López et al. 2013).

An analysis of the variation of the coal rank and the vitrinite reflectance in the Central Coal Basin shows the existence of a gradient from bituminous C coals to the north to anthracite A coals to the south (Colmenero and Prado 1993; Piedad-Sánchez et al. 2004; Colmenero et al. 2008). These results agree with KI data from the southern part of this basin, where anchizonal and epizonal values are dominant (Aller and Brime 1985; Aller et al. 1987, 2005). Subhorizontal or moderate-dipping cleavage crosscutting the main Variscan folds also appears in this southern part of the Central Coal basin (Aller 1986).

The two eastern units of the CZ (Picos de Europa and Pisuerga-Carrión units) are at the core of the arc described by the major structures (Asturian arc) and both are mutually separated by the Picos de Europa basal thrust (Fig. 1). In the Picos the Europa unit, CAI values indicate that paleotemperatures increase progressively southwards, and ancaizonal conditions are reached in the southern part of the unit (Bastida et al. 2004; Blanco-Ferrera et al. 2017) (terminology by García-López et al. 2001 is used for the metamorphic zonation from CAI data). This ancaizonal area passes without thermal discontinuity through the Picos de Europa basal thrust to the Pisuerga-Carrión unit, where diagenetic/diacaizonal and epizonal/epicaizonal areas also appear. In the latter unit, the CAI and KI values are independent of the stratigraphic position of the samples and the structural trends in the unit. The main heating episode of the CZ has been interpreted as late-Variscan, and it occurred near the Carboniferous–Permian boundary (Valín et al. 2016). The main tectonothermal event in the Pisuerga-Carrión unit was associated with the development of cleavage that crosscuts the Variscan folds. Permian and Mesozoic hydrothermal episodes, usually linked to faults, have also been recognized in this unit and in other areas of the CZ (Paniagua et al. 1993, 1996; Clauer and Weh 2014).

There is a good understanding of the tectonothermal evolution of the CZ based on CAI and/or KI data that have been synthesized by Raven and van der Pluijm (1986), García-López et al. (1999, 2007) and Bastida et al. (2002). Studies based on the coal rank distribution and vitrinite reflectance provided consistent results (Colmenero and Prado 1993; Colmenero et al. 2008). In short, the tectonothermal evolution of the CZ can be summarized as follows: (a) burial heating giving place to anchizonal/ancaizonal conditions in the basal part of some thrust units; (b) heating and development of cleavage associated with the orogenic metamorphism whose front appears near the western boundary of the CZ and extends to the hinterland; (c) late-Variscan event causing very low- or low-grade metamorphism and subhorizontal or moderate-dipping cleavage in the core of the Asturian arc and in the southern part of the Central Coal Basin; (d) contact metamorphism related to the scarce granitoid

stocks outcropping in the CZ; (e) post-Variscan hydrothermal events related to faults.

Currently, the only major unit of the CZ whose tectonothermal evolution remains elusive is the Ponga unit (Fig. 1), besides a preliminary report of García-López et al. (2017). The distribution of paleotemperatures and the analysis of the thermal events in the Ponga unit is the key to link the thermal pattern of the eastern units (Picos de Europa and Pisuerga-Carrión units) with the Central Coal Basin, which is located immediately to the west of the Ponga unit. This knowledge is also required to obtain a complete picture of the tectonothermal evolution of the CZ. The purpose of the present contribution is to assess the thermal history of the Ponga unit based on the CAI and KI methods, complemented with other previously published thermal maturity reports. In this study, samples from the Central Coal Basin in areas adjacent to the eastern and southern parts of the Ponga unit (Laviana thrust sheet) have also been considered; these are described together with those of the Ponga unit to simplify the text.

Geological setting

The Ponga unit is located next to the units that form the core of the Asturian arc (Picos de Europa and Pisuerga-Carrión units) and the Central Coal Basin (Fig. 1). Northeastwards, it becomes the Ponga–Cuera unit, a band with E–W trend in which the thrusts have the same strike as those of the Picos de Europa unit.

A synthetic stratigraphic column of the Ponga unit is shown in Fig. 2. The succession includes c. 700 m of Cambrian–Ordovician rocks of great lateral continuity, 0–10 m of uppermost Devonian rocks, and c. 1700 m of Carboniferous rocks, involving a wide hiatus from the Middle Ordovician up to the Late Devonian.

The structure of the Ponga unit consists of an E-directed imbricate thrust system and related folds that were subsequently folded by E–W trending folds (Julivert 1967a, b, 1971; Álvarez-Marrón et al. 1989; Álvarez-Marrón 1995; Del Greco et al. 2016) (Figs. 3, 4). The thrusts merge at depth into a sole thrust located at the base of the Láncara Fm (lower Cambrian) and developed in a forward sequence, giving rise to fault-bend folds associated with frontal or lateral ramps, as well as some lateral tear faults (Álvarez-Marrón 1995). A notable, later N–S shortening event caused new south-directed thrusting, reactivation of the tear faults, and amplification of folds. The evolution of the Variscan deformation generated a complex structure in the Ponga area including the development of two tectonic windows at the core of major E–W trending antiforms (Fig. 3). Subsequently, a later-Variscan extensional episode reactivated some fractures as normal faults and probably developed new

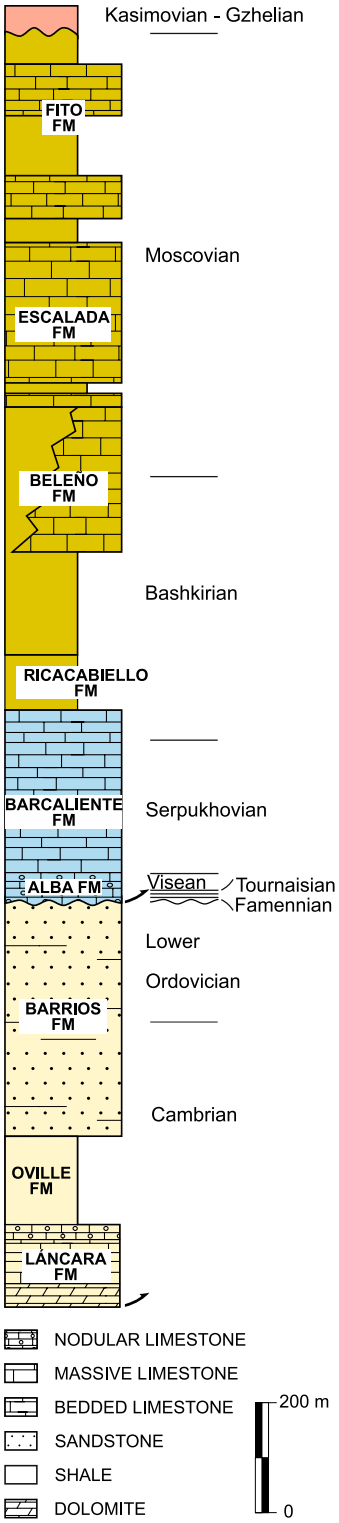

Fig. 2 Generalized stratigraphic column of the Ponga Unit (based on Álvarez-Marrón 1989, 1995)

ones in the southern part of the Ponga unit (Tornos and Spiro 2000). The most remarkable post-Variscan structure of the Ponga unit is the Ventaniella Fault (Fig. 3), which crosscuts

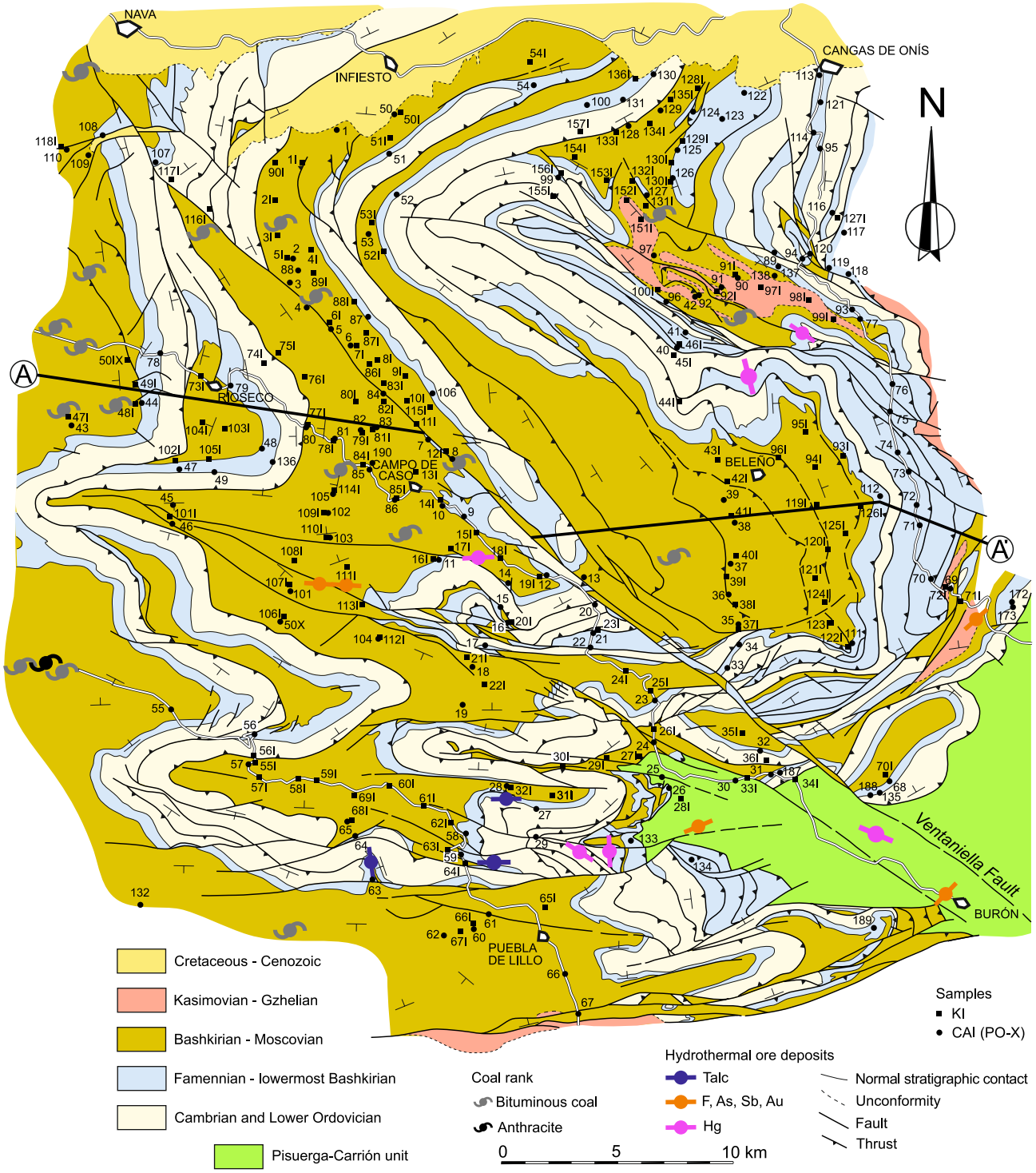

Fig. 3 Geological map of the Ponga unit showing CAI and KI sampled localities (geology modified from Álvarez-Marrón et al. 1989). Coalfields and ore deposits are from Metallogenetic Map of Mieres, Instituto Geológico y Minero de España (1975). A–A′, location of cross section of Fig. 4

the CZ with NW–SE trend. It is a dextral strike-slip fault with a net slip of 4–5 km (Julivert et al. 1971), whose activity began in the Permian and continues up to the present (López-Fernández et al. 2004).

Small igneous bodies occur in the northern part of the Ponga unit, near Infiesto (Fig. 3). These are small sills, dikes or stocks of gabbro, gabbro-diorite, granodiorite, or porphyry intruded in Pennsylvanian limestones and shales, covered in

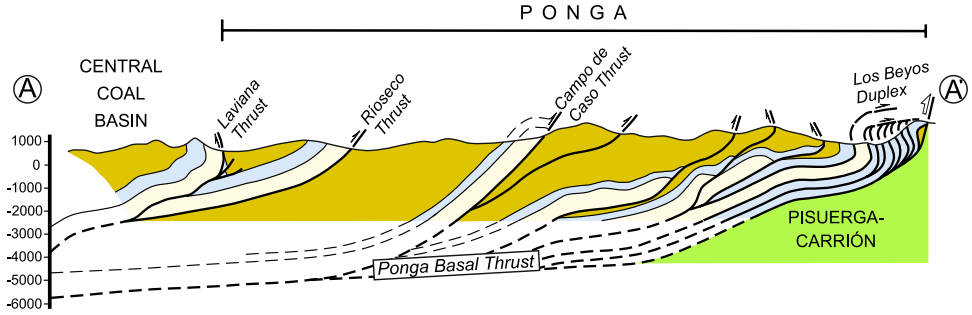

Fig. 4 Geological cross section A–A′ through the Ponga unit (modified from Álvarez-Marrón 1995)

nonconformity by Cretaceous rocks (Suárez and Marcos 1967; García Iglesias et al. 1981; Corretgé and Suárez 1990; Suárez et al. 1993). The subvolcanic intrusive complex of Infiesto provided an U–Pb age of c. 302 Ma (Valverde-Vaquero et al. 1999) and AFT ages of 143 ± 9.5 Ma (Fillon et al. 2016). The contact metamorphic aureole occupies a large area and reaches pyroxene-hornfels facies (580–610 °C), with the development of skarns and ore deposits, mainly of Cu and Au (García Iglesias et al. 1981). There are also abundant metallic ore (Cu, Hg, Fe, and Mn) and fluorite deposits in many localities of the Ponga unit (Fig. 3). In general, these deposits are epithermal and formed at temperatures between 60 and 150 °C (Loredo et al. 1988; Gutiérrez-Claverol and Luque 1993).

Important talc orebodies crop out to the N and NE of Puebla de Lillo, near the southern boundary of the Ponga unit (Fig. 3). They are hosted by hydrothermal dolostones that replace Carboniferous limestones, generally juxtaposed to Ordovician quartzites. According to Tornos and Spiro (2000), the talc is hydrothermal and formed at temperatures between 280 and 405 °C. It appears in fractured areas and it is associated with hydrothermal fluids that rose through extensional faults; the high formation temperatures suggest the existence of abnormally high thermal gradients associated with igneous rocks at depth (Tornos and Spiro 2000).

In the regional studies of the coal rank in the CZ made by Colmenero and Prado (1993) and Colmenero et al. (2008), the authors analyzed coal samples from carboniferous sedimentary units that outcrop in the study area (Fig. 3). The westernmost locations contain bituminous A, B, and C coals, and the eastern locations contain mainly bituminous C coal. Near the southern boundary of the Ponga unit, close to the León fault, an E–W narrow band with bituminous B coal crops out. These coal ranks indicate diagenetic conditions. However, in the southeastern sector of the Central Coal Basin, a wide band with anthracite B coal (anchizonal conditions) reaches up to the boundary with the study area.

Methods

Conodont Color Alteration Index

Conodonts are tooth-like apatitic remains (0.1–5 mm on average) of an extinct animal group, which was common in Cambrian-to-late Triassic oceans. They are widely used in basin analysis and hydrocarbon exploration due to their dual character as high-resolution biostratigraphic markers and thermal maturity indicators. Conodont elements experience progressive and irreversible chemical transformations of the organic matter interspersed within their phosphatic structure as a response to increasing temperature with time. Epstein et al. (1977) established the conodont Color Alteration Index (CAI) and calibrated its values on an Arrhenius plot with field collections and laboratory procedures. Rejebian et al. (1987) extended the range of the CAI to achieve metamorphic conditions. As with other thermal maturity indicators that follow the Arrhenius reactions, the CAI is progressive, cumulative, and irreversible. For the CAI metamorphic zonation, we use the terms diacaizone (CAI < 4), ancaizone ($4 \leq \text{CAI} \leq 5.5$), and epicaizone (CAI > 5), which approximately correlate with the KI domains (diagenesis/anquizone/epizone) in areas where the two indices have been used together (García-López et al. 2001). A correlation of the conodont CAI with other low-grade metamorphic indexes is shown in Table 1.

Besides the color, the textural alteration of conodonts provides hints on their diagenetic/metamorphic history. We adopt here the terminology of Rejebian et al. (1987) and García-López et al. (1997), where *smooth texture* corresponds to unaltered surfaces, *sugary texture* represents dull, frosted, and pitted surfaces (usually as a result of etching and corrosion), and *granular texture* is a result of apatite recrystallization. The different textures may

Table 1 Correlation of the conodont CAI, KI, vitrinite reflectance and coal rank from diagenesis to low-grade metamorphism (modified from Voldman et al. 2008 and references therein)

CAI	Thermal interval	CAI zone	Metapelitic zone	KI (Δ°2θ)	Maturation stage	Vitrinite reflectance Ro%	Coal rank and volatile matter (%)
1	<50-80 °C	Diacaizone	Shallow diagenetic zone		Diagenesis		Peat
1.5	50-90 °C						Lignite
							Sub-bituminous
				~1		0.60	45
2	60-140 °C		Deep diagenetic zone	~0.60	Catagenesis	1.00	C 40
						1.40	B Bituminous
3	110-200 °C						30
							A 20
				0.42		2.00	14
4	190-300 °C	Ancaizone	Low anchizone				C Semi-anthracite
				0.30	Metagenesis	3.00	
			High anchizone				B
5	300-480 °C	Epicaizone		0.25		4.00	Anthracite
			Epizone				A
6	360-550 °C					6.00	2
							Meta-anthracite
6.5	440-610 °C		Mesozone				Anthracitic
7	490-720 °C						
8	>600 °C						

cover the complete element surface or only in part. In addition, conodonts elements affected by contact metamorphism frequently exhibit a broad range of CAI values, both locally from sample to sample and even within the same sample. Hydrothermally altered conodonts may show similar CAI patterns but generally occur corroded and may present a superficial grey patina after oxidation of organic matter by the circulating fluids (Rejebian et al. 1987). Moreover, conodonts affected by metasomatic processes also tend to exhibit high CAI values but with less textural alteration and CAI variability, as observed in conodont elements recovered from carbonate turbidites intruded by mafic sills of the Yerba Loca Formation, Argentine Precordillera (Voldman et al. 2008). For recent reviews of the CAI method and other thermal maturity indexes, see, for instance, Voldman et al. (2010) and Hartkopf-Fröder et al. (2015).

In this study, we processed 147 samples from unweathered rocks in 6% acetic acid solution following the standard laboratory procedures for extracting conodonts, with 54 productive samples (Fig. 3). CAI values were determined microscopically under incident light on thin margins or lighter parts of platform conodont elements by direct comparison with a standard set obtained under the direction of A. Harris at the US Geological Survey. Samples with dispersion values ≤ 1 may either reflect the variability of the thermal conditions and/or of the intrinsic properties of the conodont elements and their host rock. In such cases, the mean CAI values were adopted. In samples with dispersion > 1, the extreme CAI values were employed instead.

The temperature ranges of the Ponga CAI values were derived from the Arrhenius plot of Epstein et al. (1977) and Rejebian et al. (1987). A minimum heating time of 10^{-3} Ma was estimated considering the time necessary to produce the CAI 5 near the Puebla de Lillo talc mine, where fluid inclusions suggest a maximum temperature of 405 °C for the ore formation (Tornos and Spiro 2000). A maximum heating time of 52 Ma is determined by the age of the youngest rocks affected by the thermal events in the adjoining Picos de Europa and Pisuerga-Carrión units (lowermost Gzhelian rocks, 304 Ma), and the oldest unconformable rocks of the CZ not thermally altered (lowermost Triassic rocks, 252 Ma) (Valín et al. 2016).

Kübler Index of illite

The Küber Index (KI) was determined in 132 samples of fine-grained clastic rocks (Fig. 3). They were prepared and analyzed by ML Valín (University of Oviedo) following the methodology described in Brime et al. (2003). These were ground and dispersed in distilled water, and the < 2 µm fraction separated by centrifugation, which was then deposited onto glass slides to obtain oriented aggregates for XRD analyses. The diffraction patterns of oriented air-dried mounts, after glycolation and after heating at 300 and 550 °C, were obtained using a Philips automated PW3200 X'Pert X-ray diffractometer using CuKα radiation and graphite monochromator. Preparation of samples and KI determination followed recommendations of the IGCP 294 working group (Kisch 1991). The KI values obtained have been converted to Kübler scale, with anchizone limits of 0.42°/0.25° Δ°2θ, using a set of samples provided by Kisch (Ben Gurion University of the Negev, Israel) and the following calibration equation:

$$KI_{Kübler} = 0.9225\ KI_{Oviedo} + 0.0263\ \left(R^2 = 0.9935\right).$$

Results

Conodont Color Alteration Index

The CAI data have a heterogeneous distribution due to the absence of limestone in some areas and the abundance of sterile samples. From the total, 54 samples yielded satisfactory results (Table 2) that display a general increase southward, and can be grouped in three E–W bands (Fig. 5). Mean CAI values range from 1.5 up to 6.6, corresponding to an interval of possible paleotemperatures from 55 to 480 °C for a heating time of 52 Ma (Table 2).

Northern band (North of Rioseco-Beleño): it is a diacaizonal band, with the exception of an ancaizonal sample (PO-50) located to the south of Infiesto. This band of low CAI values continues to the NE in the Ponga–Cuera unit (Blanco-Ferrera et al. 2011, 2017). Textures are mainly smooth and sugary except in the ancaizonal sample, which has a coarse granular texture (Table 2).

Middle band (Rioseco-Campo de Caso-Beleño band): it is a dominantly diacaizonal band, but some samples (PO-12, PO-37, PO-85, and PO-172) are ancaizonal. In addition, samples PO-71 and PO-173 located at the eastern end of the band have a wide range of CAI values and some dispersion of CAI values is locally observed between neighboring samples. Textures are sugary, except two ancaizonal samples that have granular texture (Table 2).

Southern band: it exhibits mainly ancaizonal and epicaizonal CAI values. An exceptional diacaizonal value (PO-189) is located to the west of Burón. Most of the conodonts of this band have granular texture (Table 2).

Kübler Index of illite

The KI values show dominantly diagenetic conditions, mainly in the northern and eastern parts of the Ponga unit (Fig. 6). Areas with anchizonal values are also common, though they are scarce in the northeastern sector of the unit. Three main areas with anchizonal samples are distinguished: (a) an area located to the south and southwest of Infiesto; (b) an area located close to the villages of Rioseco and Campo de Caso; (c) a sector located to the northwest of Puebla de Lillo.

Interpretation

The distribution of the KI values is irregular and appears to be independent of the stratigraphic position of the samples and of the main structures of the Ponga unit. Changes in KI values are not appreciated across thrusts or other types of faults (Fig. 6). For example, Cambrian samples (45I and 56I) located in the basal part of two thrust sheets have similar diagenetic KI values than their adjacent Carboniferous samples located in the footwall near the thrust (46I and 55I, respectively). This indicates that there is not thermal jump through the thrusts. Although the number and the stratigraphic range of CAI samples are smaller than those of KI samples (with exception of the Famennian sample PO-172, all CAI samples are Carboniferous), the distribution of CAI values (Fig. 5; Table 2) is also independent of the stratigraphic position of the samples, indicating that the maximum temperatures reached by the host rocks are not controlled by sedimentary burial.

Comparison of the KI and CAI value distributions shows some differences between them. The CAI distribution and the textures of the conodonts allow the recognition of three E–W bands, with increasing metamorphism to the south of the Ponga unit. The KI distribution also suggests higher metamorphic grade in the southern part, although with discrepancies with the CAI distribution that are found mainly in the middle band.

The ancaizonal, epicaizonal, and anchizonal values in the Ponga unit are probably related to hot fluids ascending through faults as suggested by: (a) the numerous hydrothermal dolostones and ore-related deposits (Gutierrez-Claverol and Luque 1993; Tornos and Spiro 2000), (b) the common wide range of CAI values within a sample and between nearby localities, and (c) the existence of E–W trending extensional faults in the southern half part of the study area (Álvarez-Marrón 1995). The hydrothermal processes would have generated a heterogeneous heating increasing towards the south, involving high thermal gradients of local character. Therefore, the CAI or KI in a specific locality should depend on the heat provided by the hydrothermal fluid, the duration of the thermal event, the distance of the sample to the heat source, and the thermal conductivity and fluid content of the involved rocks.

Discrepancies between CAI and KI values can be ascribed to the different kinetics of the illitization and maturation of organic matter, as the former process is less sensitive to the time spent at a certain temperature (Hillier et al. 1995; Brime et al. 2001; Árkai et al. 2002; Aller et al. 2005). Another possible cause of divergence between CAI and KI values is retrograde metamorphism of clay minerals (e.g., Voldman et al. 2008). If several events with different temperatures occur, the CAI value tends to reflect the highest temperature event. The existence of several thermal events has been highlighted by Tornos and Spiro (2000) to explain the development of dolostone and ore bodies of talc of Puebla de Lillo; these authors distinguish four hydrothermal events. The temperature of the highest-grade event was between 280 and 405 °C, which nearly exactly coincides

Table 2 Conodont CAI values from the Ponga unit and temperatures inferred from the CAI Arrhenius plot (Epstein et al. 1977; Rejebian et al. 1987)

Sample	Stratigraphic unit	Age	CAI (number of specimens)	Mean CAI value	Temperature range (°)	Texture
PO-3	Escalada Fm	Moscovian	3 (2)	3	120–230	Smooth bright, faint sugary
PO-7	Barcaliente Fm	Serpukhovian	2 (2)	2	55–155	Sugary
PO-8	Barcaliente Fm	Serpukhovian	1.5 (1)	1.5	< 125	Faint sugary
PO-10	Barcaliente Fm	Serpukhovian	2 (1)	2	55–155	Smooth bright
PO-12	Barcaliente Fm	Bashkirian	4 (3)	4	190–300	Sugary, dispersed organic matter
PO-14	Barcaliente Fm	Bashkirian	2 (6)	2	55–155	Smooth bright
PO-16	Barcaliente Fm	Bashkirian	2 (6)	2	55–155	Granular, corrosion, overgrowth
PO-22	Barcaliente Fm	Serpukhovian	3 (1)	3	120–230	Granular, corrosion, overgrowth
PO-25	Olistolith	Serpukhovian	4 (4)	4	190–300	Sugary
PO-26	Alba Fm	Visean	4.5 (34)	4.5	240–350	Sugary
PO-30	Pando Gr	Moscovian	5.5 (2)	5.5	340–440	Granular, faint recrystallization
PO-31	Barcaliente Fm	Bashkirian	5.5 (2)	5.5	340–440	Granular, faint recrystallization
PO-32	Alba Fm	Visean	5.5 (101), 5.5–6 (50)	5.6	345–445	Granular, faint recrystallization, cleavage
PO-37	Escalada Fm	Moscovian	4 (2)	4	190–300	Sugary
PO-38	Escalada Fm	Moscovian	3 (1)	3	120–230	Sugary
PO-39	Escalada Fm	Moscovian	3.5 (13)	3.5	155–265	Cleavage
PO-41	Alba Fm	Visean	2 (1)	2	55–155	Smooth bright
PO-44	Barcaliente Fm	Bashkirian	3.5 (2)	3.5	155–265	Sugary, corrosion, dispersed organic matter
PO-45	Escalada Fm	Moscovian	2.5–3 (7)	2.75	100–210	Sugary
PO-48	Barcaliente Fm	Bashkirian	1.5 (4)	1.5	< 125	Faint sugary
PO-50	Escalada Fm	Moscovian	4 (2)	4	190–300	Granular
PO-55	Lena Gr	Moscovian	4.5 (2)	4.5	240–350	Smoke, grey patina
PO-56	Alba Fm	Visean	6.5 (3), 7 (1)	6,6	385–480	Granular
PO-58	Barcaliente Fm	Serpukhovian	5 (5)	5	305–405	Granular
PO-69	Beleño Fm	Bashkirian	2 (1)	2	55–155	Faint sugary
PO-71	Alba Fm	Visean	2 (1), 4.5 (1)	–	–	Sugary, corrosion, overgrowth
PO-74	Barcaliente Fm	Serpukhovian	3 (2)	3	120–230	Smooth bright
PO-79	Barcaliente Fm	Serpukhovian	2 (2)	2	55–155	Faint sugary
PO-82	Escalada Fm	Moscovian	3 (1)	3	120–230	Smooth bright
PO-85	Fito Fm	Moscovian	4 (1), 5 (5)	4.8	285–395	Granular
PO-91	Escalada Fm	Moscovian	2 (1)	2	55–155	Smooth bright
PO-93	Alba Fm	Visean	2 (10)	2	55–155	Smooth bright
PO-99	Alba Fm	Visean	1.5 (11)	1.5	< 125	Smooth bright
PO-109	Lena Gr	Moscovian	3 (2)	3	120–230	Faint sugary
PO-110	Lena Gr	Moscovian	2 (1)	2	55–155	Sugary, grey patina
PO-117	Alba Fm	Visean	2.5 (3)	2.5	80–190	Sugary, pink patina
PO-120	Barcaliente Fm	Serpukhovian	1.5 (1)	1.5	< 125	Sugary, overgrowth
PO-127	Barcaliente Fm	Bashkirian	2 (2)	2	55–155	Sugary
PO-132	Lena Gr	Moscovian	5–5.5 (3)	5.25	320–420	Granular
PO-133A	Alba Fm	Visean	4.5 (1), 5 (2), 5–5.5 (3)	5	305–405	Sugary, granular
PO-133B	Barcaliente Fm	Serpukhovian	5–5.5 (1)	5.25	320–420	Granular
PO-134A	Ermita Fm	Tournaisian	4 (1)	4	190–300	Granular, faint recrystallization
PO-134B	Alba Fm	Visean	4 (2)	4	190–300	Granular, faint recrystallization
PO-135	Alba Fm	Visean	5–5.5 (1), 6 (2)	5.75	360–460	Granular
PO-136A	Alba Fm	Serpukhovian	2 (4), 3 (2)	2.3	70–175	Sugary
PO-136B	Escalada Fm	Moscovian	1.5 (2), 2 (8), 2.5 (1)	2	55–155	Sugary, grey patina

Table 2 (continued)

Sample	Stratigraphic unit	Age	CAI (number of specimens)	Mean CAI value	Temperature range (°)	Texture
PO-136C	Fito Fm	Moscovian	1.5 (1), 2 (1)	1.75	50–140	Faint sugary
PO-137	Barcaliente Fm	Bashkirian	2 (2), 2.5 (2), 3 (7), 3.5 (2)	–	–	Sugary, grey patina
PO-138	Escalada Fm	Moscovian	2 (1), 2.5 (3), 3 (5)	2.7	95–205	Sugary, grey patina
PO-172	Ermita Fm	Famennian	5 (2)	5	305–405	Granular
PO-173	Alba Fm	Visean	4.5 (1), 5 (1), 6 (1), 7 (2)	–	–	Sugary
PO-187	Alba Fm	Visean	5.5 (2)	5.5	340–440	Granular
PO-188	Alba Fm	Visean	4 (7), 4.5 (5), 5-5.5 (1), 6 (2)	–	–	Sugary
PO-189	Barcaliente Fm	Bashkirian	2 (5), 3 (2)	2.2	65–170	Sugary

with the temperature span required to reach the CAI of 5 of the nearest sample (PO-58, Table 2).

The anchizonal and ancaizonal values of samples located to the south of Infiesto, in the northern sector of the Ponga (Figs. 5, 6), are ascribed to a short-term heating event produced by the late-Variscan igneous rocks that crop out in the area.

Discussion: the metamorphism of the Ponga unit in the regional context

The CAI, KI, and coal rank results shown in Fig. 7 indicate that the very low-to-low-grade metamorphism located in the southern Ponga area is part of a major E–W band that crosscuts the main Variscan structures in the eastern CZ. This involves a southwards increase of the metamorphic grade in all the units, in some cases with a thermal gradient well defined, such as that shown by the coal rank and vitrinite reflectance in the Central Coal Basin (Piedad-Sánchez et al. 2004; Colmenero et al. 2008) and by CAI data in the Picos de Europa unit (Blanco-Ferrera et al. 2017). The width of this band appears to be narrower in the Ponga unit, while it covers large areas of the Pisuerga-Carrión and Valsurvio units to the east and of the Central Coal Basin to the west (Fig. 1). Both in the Ponga unit and in the Central Coal Basin, the metamorphic band ends abruptly to the south, against the León Fault. However, in the Pisuerga-Carrión unit, low-grade metamorphic rocks crop out to the south of the fault, probably reflecting a post-Variscan reactivation movement of the León Fault, with uplifting of the northern fault block (e.g., Alonso et al. 2007).

A considerable difference between the Ponga unit and its adjacent units is relative to the cleavage development. In the Central Coal Basin and the Pisuerga-Carrión and Valsurbio units, there is subhorizontal or moderately dipping cleavage crosscutting the main Variscan folds. This cleavage has not been found in the Ponga unit, despite its metamorphic grade being similar. This may be suggesting less strain during the late-Variscan extensional deformation, which does not affect the CAI response.

The very low-to-low-grade metamorphic E–W band has been interpreted as a result of an extensional late-Variscan episode in the units adjacent to the Ponga unit (Aller et al. 2005; Valín et al. 2016). This interpretation is supported in the Ponga unit by the hydrothermal ore bodies of talc and extensional faults (Álvarez-Marrón 1989, 1995; Tornos and Spiro 2000). The presence of igneous rocks at depth in the southern part of the Ponga unit has been suggested by Tornos and Spiro (2000) and by Valín et al. (2016) in the Pisuerga-Carrión unit, where small outcrops of intrusive rocks are common. In the La Sobia-Bodón units, south of the León Fault, the positive temperature anomalies broadly correlate with hydrothermal dolostones and ore mineralizations (Honlet et al. 2017).

The age of the extensional event can be constrained by the U–Pb age of the granodiorite stock of Peña Prieta in the Pisuerga-Carrión unit (292 + 2/− 3; Valverde-Vaquero et al. 1999), which is post-tectonic with respect to the subhorizontal cleavage (Gallastegui et al. 1990; Rodríguez Fernández 1994). According to these data, the extensional thermal event took place near the Carboniferous–Permian boundary and progressed during the Cisuralian with the intrusion of many small igneous bodies along faults. Since the subhorizontal cleavage associated with the tectonothermal extensional event cuts the Variscan folds whose last tightening is associated with the close of the Asturian arc, this event was subsequent to the closure of the arc. The age (c. 302 Ma) estimated by Valverde-Vaquero et al. (1999) for the Infiesto's igneous rocks is slightly older than that of the Peña Prieta granodiorite, suggesting that the latter may correspond with an earlier stage of the extensional episode.

The distribution of paleotemperatures in the Ponga unit is not stratigraphically controlled in the Ponga unit. This is in contrast to what happens in the western and southern units of the CZ, where thrust units increase their metamorphic grade towards their base (Bastida et al. 1999; Brime et al. 2001; Aller et al. 2005, García-Lopez

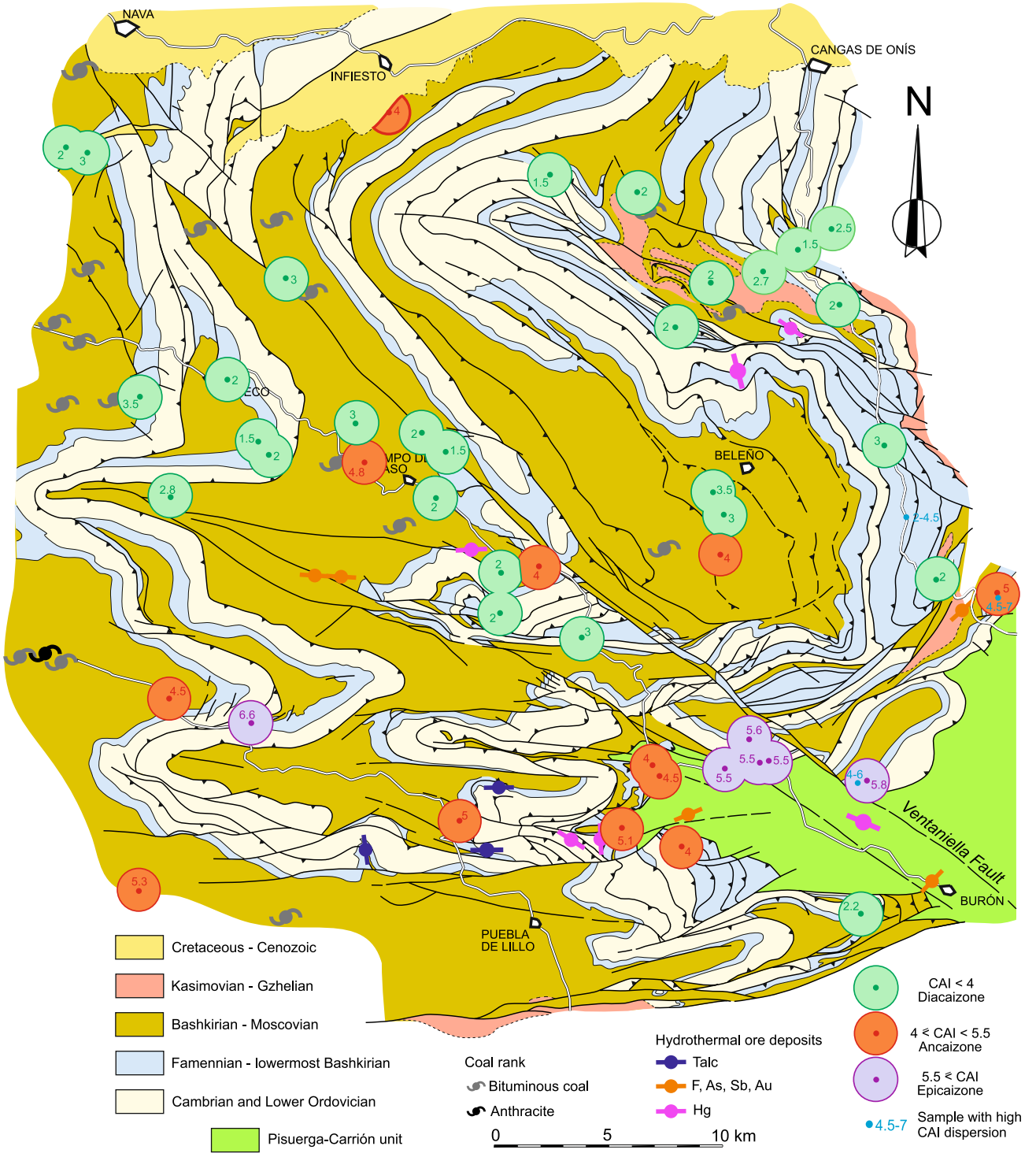

Fig. 5 Geological map of the Ponga unit showing the location of mean CAI values (geology adapted from Álvarez-Marrón et al. 1989). The colored circles have been drawn to better visualize the metamorphic grade of the corresponding sample

et al. 2013). This is probably due to the thinner pre-Carboniferous stratigraphic succession of the Ponga unit. The absence of metamorphism related to tectonic overburden also denotes limited superposition and/or rapid exhumation, similar to what is observed in other areas of the CZ, such as in the Esla unit (García-López et al. 2013).

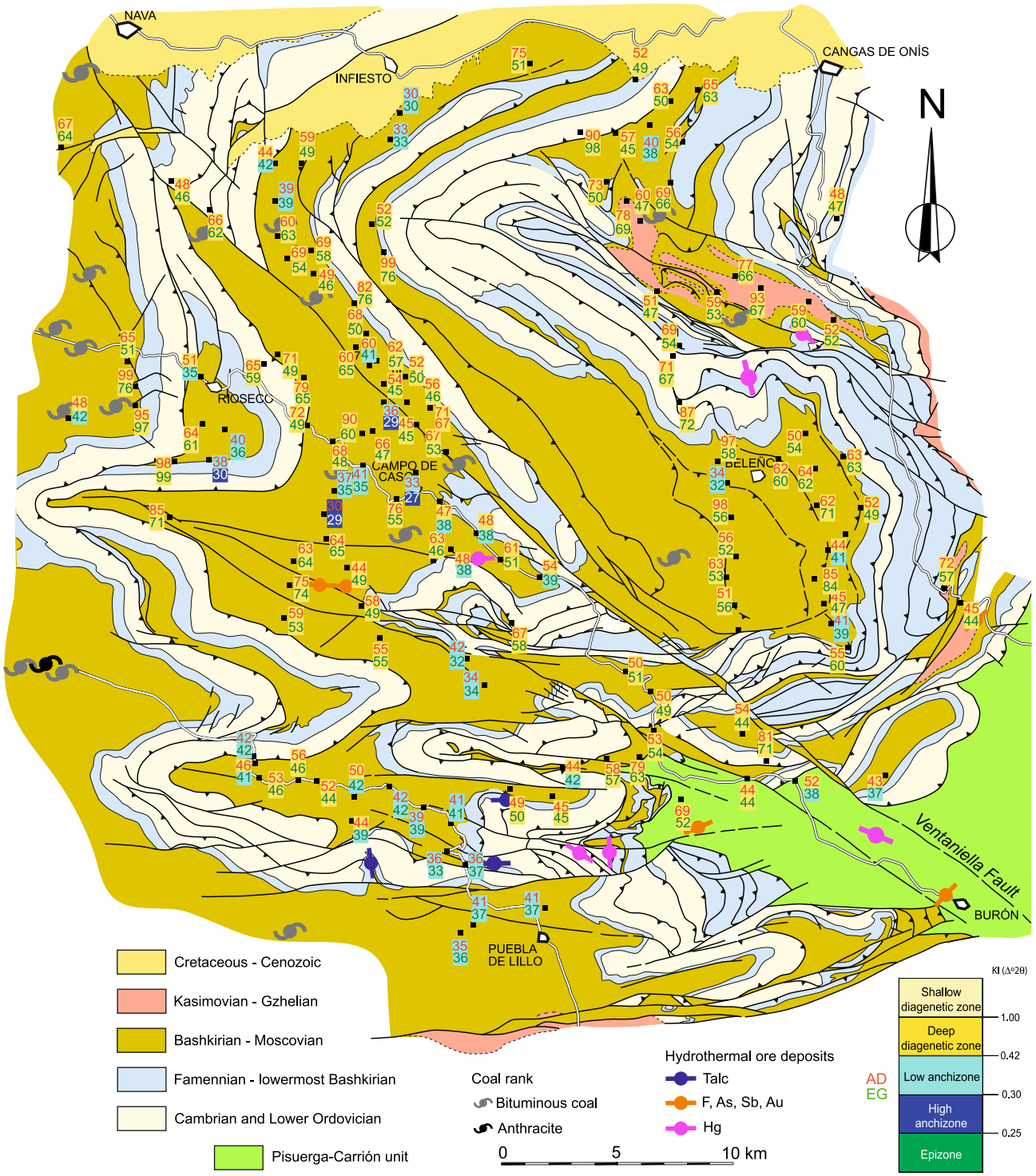

Fig. 6 Geological map of the Ponga unit showing the location of Kübler index (KI) values (×100) (Kübler scale). Upper value, in red, is the air-dried sample; lower value, in green, is the ethylene glycol-treated sample. Geology adapted from Álvarez-Marrón et al. (1989)

Conclusions

This study aims to complete the paleothermometric framework of the CZ, an arcuate fold and thrust belt where burial, orogenic, hydrothermal, and contact thermal events have been identified. The distribution of CAI and KI values in the Ponga unit shows the existence of a southern area with very low-to-low-grade metamorphism. The thermal

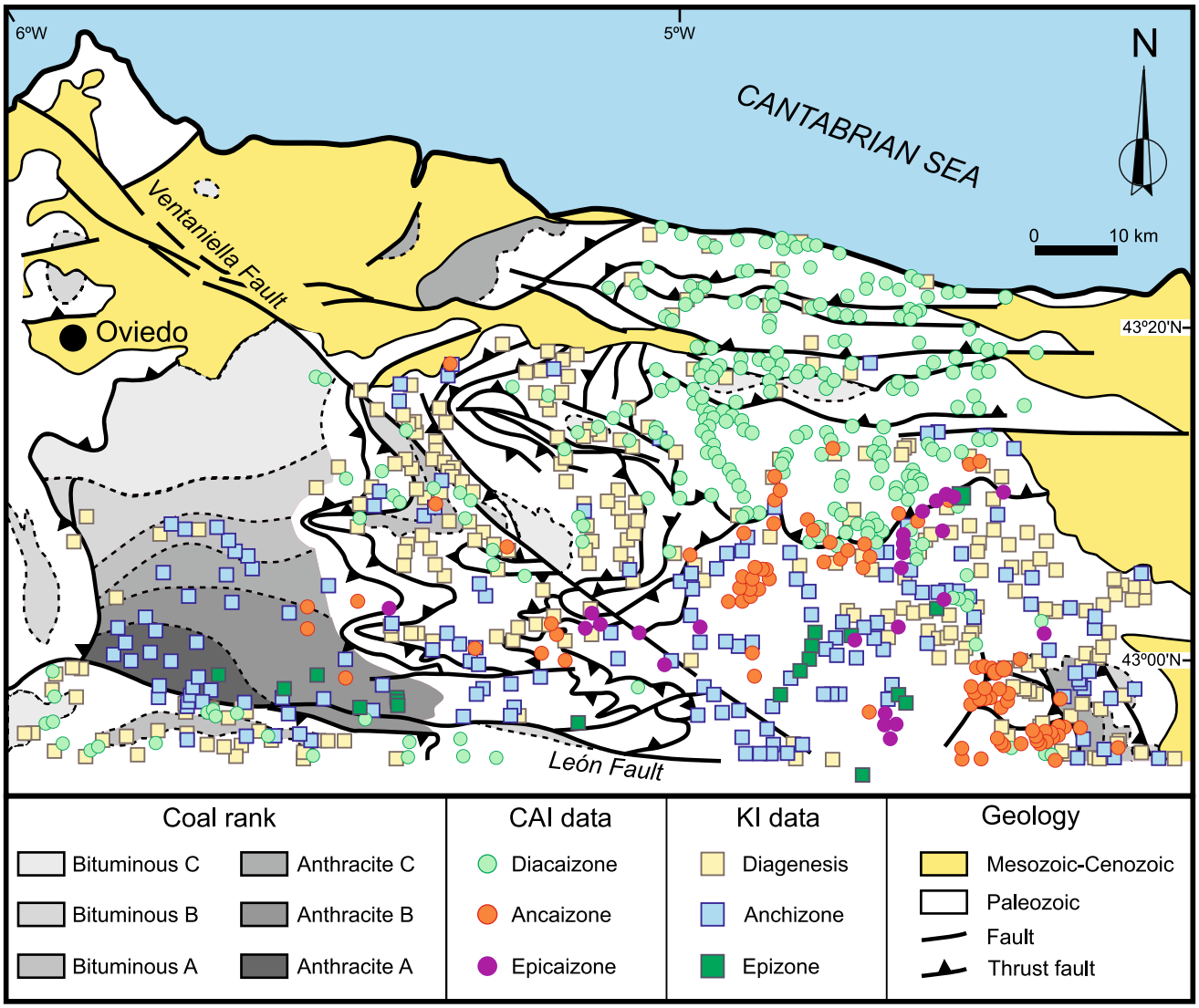

Fig. 7 CAI, KI, and coal rank data obtained for several authors for the Ponga unit and adjacent units to the east (Picos de Europa and Pisuerga-Carrión units) and to the west (Central Coal Basin) (compiled from Aller and Brime 1985; Aller 1986; Bastida et al. 2004; Aller et al. 2005; Colmenero et al. 2008; Blanco-Ferrera et al. 2011, 2017; Valín et al. 2016; and this study). Notice the southward increase of the coal rank that reaches up to Antracite A in the Central Coal Basin, and also the samples in Epicaizone in the east, some near the Picos de Europa frontal thrust

event that produced this metamorphism is interpreted as related to hydrothermal fluids generated from deep igneous intrusions; magma and fluids ascending through late-Variscan extensional faults. This heterogeneous heating system is responsible of high local thermal gradients and discrepancies between the CAI and KI values.

The southern metamorphic area in the Ponga unit is part of a major E–W band that runs along the southern part of the CZ. The metamorphism is interpreted to be related to a late-Variscan gravitational instability of the orogenic belt that has given rise to extensional deformation. This tectonothermal event appears to postdate the closure of the Asturian arc.

The short-term heating event in the northern part of the Ponga unit, associated with the Infiesto's igneous rocks, can be an early local manifestation of the same Variscan extensional episode.

Acknowledgements We profoundly appreciate Dr. María Luz Valín (University de Oviedo) for helping us with the KI data; she prepared and analyzed the samples. Dr. J. Álvarez Marrón (ICTJA-CSIC) is greatly appreciated for her critical review. G. Voldman thanks CONICET, the Universidad de Oviedo and Banco Santander for a visiting fellowship. The present paper has been supported by the

CGL2015-66997-R project funded by the Ministerio de Economía y Competitividad of Spain.

References

Aller J (1986) La estructura del sector meridional de las unidades del Aramo y Cuenca Carbonífera Central. Servicio de Publicaciones del Principado de Asturias, Spain, pp 1–180

Aller J, Brime C (1985) Deformación y metamorfismo en la parte Sur de la Cuenca Carbonífera Central (NO de España), vol 3. Compte Rendu X Congrès International Stratigraphie et de Géologie du Carbonifère, Madrid, pp 541–548

Aller J, Bastida F, Brime C, Pérez-Estaún A (1987) Cleavage and its relation with metamorphic grade in the Cantabrian Zone (Hercynian of North-West Spain). Sci Géol Bull 40:255–272

Aller J, Valín ML, García-López S, Brime C, Bastida F (2005) Very low grade metamorphic episodes in the southern Cantabrian Zone (Iberian Variscan belt, NW Spain). Bull Soc Géol France 176:487–498

Alonso JL, Martínez Abad I, García-Ramos JC (2007) Nota sobre la presencia de una sucesión cretácica en el Macizo de Las Ubiñas (Cordillera Cantábrica). Implicaciones tectónicas y geomorfológicas. Geogaceta 43:47–50

Álvarez-Marrón J (1989) La estructura geológica de la región del Ponga (Zona Cantábrica, NW de España). Unpub. PhD. Thesis, Univ. Oviedo, p 223

Álvarez-Marrón J (1995) Three-dimensional geometry and interference of fault-bend folds: examples from the Ponga Unit, Variscan belt, NW Spain. J Struct Geol 17:549–560

Álvarez-Marrón J, Heredia N, Pérez-Estaún A (1989) Mapa geológico de la región del Ponga. Trabajos Geol 18:127–135

Árkai P, Ferreiro Mählmann R, Suchý V, Balogh K, Sýkorova I, Frey M (2002) Possible effects of tectonic shear strain on phyllosilicates: a case study from the Kandersteg area, Helvetic domain, Central Alps, Switzerland. Schweiz Mineral Petrogr Mitt 82:273–290

Bastida F, Brime C, García-López S, Sarmiento GN (1999) Tectonothermal evolution in a region with thin skinned tectonics: the western nappes in the Cantabrian Zone (Variscan belt of NW Spain). Int J Earth Sci 88:38–48

Bastida F, Brime C, García-López S, Aller J, Valín ML, Sanz-López J (2002) Tectono-thermal evolution of the Cantabrian Zone. In: García-López S, Bastida F (eds) Palaeozoic conodonts from northern Spain. Inst Geol Min España, serie Cuadernos del Museo Geominero 1, pp 105–123

Bastida F, Blanco-Ferrera S, García-López S, Sanz-López J, Valín ML (2004) Transition from diagenesis to metamorphism in a calcareous tectonic unit of the Iberian Variscan belt (Central massif of the Picos de Europa, NW Spain). Geol Mag 141:617–628

Blanco-Ferrera S, Sanz-López J, García-López S, Bastida F, Valín ML (2011) Conodont alteration and tectonothermal evolution of a diagenetic unit in the Iberian Variscan belt (Ponga-Cuera unit, NW Spain). Geol Mag 148:35–49

Blanco-Ferrera S, Sanz-López J, García-López S, Bastida F (2017) Tectonothermal evolution of the northeastern Cantabrian Zone (Spain). Int J Earth Sci. https://doi.org/10.1007/s00531-016-1365-5

Brime C, García-López S, Bastida F, Valín ML, Sanz-López J, Aller J (2001) Transition from diagenesis to metamorphism near the front of the Variscan regional metamorphism (Cantabrian Zone, Northwestern Spain). J Geol 109:363–379

Brime C, Talent JA, Mawson R (2003) Low-grade metamorphism in the Paleozoic sequence of the Townsville hinterland, northeastern Australi. Aust J Earth Sci 50:751–767

Clauer N, Weh A (2014) Time constraints for the tectono-thermal evolution of the Cantabrian Zone in NW Spain by illite K–Ar dating. Tectonophysics 623:39–51

Colmenero JR, Prado JG (1993) Coal basins in the Cantabrian Mountains, Northwestern Spain. Int J Coal Geol 23:215–229

Colmenero JR, Suárez-Ruiz I, Fernández-Suárez J, Barba P, Llorens T (2008) Genesis and rank distribution of upper carboniferous coal basins in the Cantabrian Mountains, Northern Spain. Int J Coal Geol 76:187–204

Corretgé LG, Suárez O (1990) Igneous rocks of the Cantabrian/Palentian Zone. In: Dallmeyer RD, Martínez García E (eds) Premesozoic geology of Iberia. Springer, Berlin, pp 72–79

Del Greco K, Johnston ST, Gutiérrez-Alonso G, Shaw J, Fernández Lonzano J (2016) Interference folding and orocline implications: a structural study of the Ponga Unit, Cantabrian orocline, northern Spain. Lithosphere 8(6):757–768

Epstein AG, Epstein JB, Harris LD (1977) Conodont color alteration—an index to organic metamorphism. US Geol Surv Prof Pap 995:G1–G27

Fillon C, Pedreira D, van der Beek PA, Huismans RS, Barbero L, Pulgar JA (2016) Alpine exhumation of the central Cantabrian Mountains, Northwest Spain. Tectonics. https://doi.org/10.1002/2015TC004050

Gallastegui G, Heredia N, Rodríguez Fernández LR, Cuesta A (1990) El "stock" de Peña Prieta en el contexto del magmatismo de la Unidad del Pisuerga-Carrión (Zona Cantábrica, Nde España). Cad Lab Xeol Laxe 15:203–215

García Iglesias J, Gutiérrez Claverol M, Orueta J, Suárez O (1981) Mineralizaciones asociadas al metamorfismo de contacto del complejo ígneo de Infiesto (Zona oriental de Asturias, España). Publ Mus Lab Miner Geol Fac. Cien Oporto CXI:155–181

García-López S, Brime C, Bastida F, Sarmiento GN (1997) Simultaneous use of thermal indicators to analyse the transition from diagenesis to metamorphism: an example from the Variscan Belt of northwest Spain. Geol Mag 134:323–334

García-López S, Bastida F, Brime C, Aller J, Valín ML, Sanz-López J, Méndez CA, Menéndez-Álvarez JR(1999) Los episodios metamórficos de la Zona Cantábrica y su contexto estructural. Trabajos de Geología21:177–187

García-López S, Bastida F, Aller J, Sanz-López J (2001) Geothermal paleogradients and metamorphic zonation from the conodont colour alteration index (CAI). Terra Nova 13:79–83

García-López S, Brime C, Valín ML, Sanz-López J, Bastida F, Aller J, Blanco Ferrera S (2007) Tectonothermal evolution of a foreland fold and thrust belt: the Cantabrian Zone (Iberian Variscan belt, NW Spain). Terra Nova 19:469–475

García-López S, Bastida F, Aller J, Sanz-López J, Marín JA, Blanco Ferrera S (2013) Tectonothermal evolution of a major thrust system: the Esla–Valsurbio unit (Cantabrian Zone, NW Spain). Geol Mag 150:1047–1061

García-López S, Voldman GG, Bastida F, Aller J (2017) Tectonothermal analysis of a major unit of the Cantabrian Zone (Variscan belt, NW Spain) using conodont color alteration index. In: Liao JC, Valenzuela-Ríos JI (eds) 4th international conodont symposium "Progress on Conodont investigation", Valencia (Spain). Cuadernos del Museo Geominero, vol 22, pp 229–334

Gutiérrez Claverol M, Luque C (1993) Recursos del subsuelo de Asturias. Servicio de Publicaciones de la Universidad de Oviedo, Oviedo, pp 1–392

Gutiérrez-Alonso G, Nieto F (1996) White-mica 'crystallinity', finite strain and cleavage development across a large Variscan structure, NW Spain. J Geol Soc Lond 153:287–299

Hartkopf-Fröder C, Königshof P, Littke R, Schwarzbauer J (2015) Optical thermal maturity parameters and organic geochemical alteration at low grade diagenesis to anchimetamorphism: a review. Int J Coal Geol 150–151:74–119

Hillier S, Matyas J, Matter A, Vasseur G (1995) Illite/smectite diagenesis and its variable correlation with vitrinite reflectance in the Pannonian basin. Clays Clay Min 43:174–183

Honlet R, Gasparrini M, Jäger H, Muchez Ph, Swennen R (2017) Precursor and ambient rock paleothermometry to assess the thermicity of burial dolomitization in the southern Cantabrian Zone (northern Spain). Int J Earth Sci. https://doi.org/10.1007/s00531-017-1541-2

Instituto Geológico y Minero de España (1975) Mapa Metalogenético de España 1:200,000. Mieres. Ministerio de Industria, Servicio de Publicaciones

Julivert M (1967a) La ventana tectónica del río Color y la prolongación septentrional del manto del Ponga. Trabajos Geol 1:1–26

Julivert M (1967b) La ventana del río Monasterio y la terminación meridional del manto del Ponga. Trabajos Geol 1:47–58

Julivert M (1971) Décollement tectonics in the Hercynian Cordillera of NW Spain. Am J Sci 270:1–29

Julivert M (1978) Hercynian orogeny and Carboniferous paleogeography in Northwestern Spain: a model of deformation-sedimentation relationships. Z Deut Geol Gesellschaft 129:565–592

Julivert M, Ramírez del Pozo J, Truyols J (1971) Le réseau de failles et la couverture por-Hercynienne dans les Asturies. In: Histoire structurale du Golfe de Gascogne, 1. Publications de l'Institute Français du Pétrole, Ed. Technip, Paris, pp 1–28

Kisch HJ (1991) Illite crystallinity: recommendations on sample preparation, X-ray diffraction settings and interlaboratory settings. J Metamorph Geol 9:665–670

López-Fernández C, Pulgar JA, Glez-Cortina JM, Gallart J, Díaz J, Ruiz M (2004) Actividad sísmica en el noroeste de la Península Ibérica observada por la red sísmica local del Proyecto GASPI (1999–2002). Trabajos Geol 24:91–106

Loredo J, Luque C, García Iglesias J (1988) Conditions of formation of mercury deposits from the Cantabrian Zone (NW Spain). Bull Minér 111:393–400

Marcos A, Pulgar JA (1982) An approach to the tectonostratigraphic evolution of the Cantabrian foreland thrust and fold belt, Hercynian Cordillera of NW Spain. Neues Jahrb Geol P A 163:256–260

Paniagua A, Fontboté L, Fenoll P, Fallick AE, Moreiras DB, Corretgé LG (1993) Tectonic setting, mineralogical characteristics and age dating of a new type of epithermal carbonate-hosted, precious metal-five element deposits: the Villamanín Area (Cantabrian Zone, Northern Spain). In: Fenoll Hach-Ali P, Torres-Ruiz J, Gervilla F (eds) Current research in geology applied to ore deposits. 2nd biennial Society for Geology Applied to Mineral Deposits (SGA) Meeting, Granada, pp 531–534

Paniagua A, Rodríguez Pevida LS, Loredo J, Fontboté L, Fenoll Hach-Alí P (1996) Un yacimiento de Au en carbonatos del Orógeno Hercínico: el área de Salamón (N León). Geogaceta 20:1605–1608

Pérez-Estaún A (1978) Estratigrafía y estructura de la rama Sur de la Zona Asturoccidental-leonesa. Mem Inst Geol Min Esp 92:1–144

Piedad-Sánchez N, Izart A, Martínez L, Suárez-Ruiz I, Elie M, Menetrier C (2004) Paleothermicity in the Central Asturian Coal Basin, North Spain. Coal Geol 58:205–229

Raven JGM, van der Pluijm BA (1986) Metamorphic fluids and transtension in the Cantabrian Mountains of northern Spain: an application of the conodont colour alteration index. Geol Mag 123:673–681

Rejebian VA, Harris AG, Huebner JS (1987) Conodont color and textural alteration: an index to regional metamorphism and hydrothermal alteration. Geol Soc Am Bull 99:471–479

Rodríguez Fernández LR (1994) La estratigrafía del Paleozoico y la estructura de la región de Fuentes Carrionas y áreas adyacentes (Cordillera herciniana, NO de España). Cad Lab Xeol Laxe Serie Nova Terra 9:1–240

Suárez O, Marcos A (1967) Sobre las rocas ígneas de la región de Infiesto. Trabajos Geol 1:165–173

Suárez O, Cuesta A, Gallastegui G, Corretgé LG (1993) Mineralogía y petrología de las rocas plutónicas de Infiesto (Zona Cantábrica, N de España). Trabajos Geol 19:123–153

Tornos F, Spiro BF (2000) The geology and isotope Geochemistry of the Talc Deposits of Puebla de Lillo (Cantabrian Zone, Northern Spain). Econ Geol 95:1277–1296

Valín ML, García-López S, Brime C, Bastida F, Aller J (2016) Tectonothermal evolution in the core of an arcuate fold and thrust belt: the south-eastern sector of the Cantabrian Zone (Variscan belt, north-western Spain). Solid Earth 7:1003–1022

Valverde-Vaquero P, Cuesta A, Gallastegui G, Suárez O, Corretgé LG, Dunning GR (1999) U–Pb dating of Late Variscan magmatism in the Cantabrian Zone (Northern Spain). European Union of Geosciences conference (EUG 10), Strasbourg, France. J Conf Abstr 4:101

Voldman GG, Albanesi GL, Do Campo M (2008) Conodont palaeothermometry of contact metamorphism in Middle Ordovician rocks from the Precordillera of western Argentina. Geol Mag 145(4):449–462

Voldman GG, Bustos-Marún RA, Albanesi GL (2010) Calculation of the conodont Color Alteration Index (CAI) for complex thermal histories. Int J Coal Geol 82(1–2):45–50